1662 J. Med. Chem. 2010, 53, 1662–1672
DOI: 10.1021/jm901386e

Journal of Medicinal Chemistry Article

Discovery of Novel Fibroblast Growth Factor Receptor 1 Kinase Inhibitors by Structure-Based Virtual Screening†

Krishna P. Ravindranathan,‡ Valsan Mandiyan,§ Anil R. Ekkati,‡ Jae H. Bae,§ Joseph Schlessinger,§ and William L. Jorgensen*,‡

‡Department of Chemistry, Yale University, New Haven, Connecticut 06520, and §Department of Pharmacology, Yale University School of Medicine, New Haven, Connecticut 06520

Received September 17, 2009

Fibroblast growth factors (FGFs) play important roles in embryonic development, angiogenesis, wound healing, and cell proliferation and differentiation. In search of inhibitors of FGFR1 kinase, 2.2 million compounds were docked into the ATP binding site of the protein. A co-crystal structure, which shows two alternative conformations for the nucleotide binding loop, is reported. Docking was performed on both conformations and, ultimately, 23 diverse compounds were purchased and assayed. Following hit validation, two compounds **10** and **16**, a benzylidene derivative of pseudothiohydantoin and a thienopyrimidinone derivative, respectively, were discovered that inhibit FGFR1 kinase with IC_{50} values of 23 and 50 μM. Initial optimization of **16** led to the more unsaturated **40**, which has significantly enhanced potency, 1.9 μM. The core structures represent new structural motifs for FGFR1 kinase inhibitors. The study also illustrates complexities associated with the choice of protein structures for docking, possible use of multiple kinase structures to seek selectivity, and hit identification.

Introduction

Protein tyrosine kinases play an important role in the signaling pathways that control cell proliferation and differentiation. Enhanced protein kinase activity due to activating mutations or overexpression has been implicated in many cancers.[1−3] The fibroblast growth factor receptors (FGFR1[a] through FGFR4)[4] play an important role in embryonic development, angiogenesis, wound healing, and malignant transformation.[5] In response to growth factor stimulation, these transmembrane receptors undergo ligand dependent dimerization, which activates their intracellular tyrosine kinase domains, resulting in autophosphorylation and subsequent interaction with and recruitment of downstream cellular target proteins.[6] Inappropriate activation of FGF receptors have been implicated in several angiogenic pathologies including diabetic retinopathy, rheumatoid arthritis, atherosclerosis, and tumor neovascularization.[7−9] Aberrant FGFR kinase activity has been implicated in different cancers including breast cancer,[10−15] human pancreatic cancer,[16] astrocytomas,[17,18] salivary gland adenosarcoma,[19] Kaposi's sarcoma,[20] ovarian cancer,[21] and prostate cancer.[22,23] In addition, activating mutations in FGFR genes have been associated with various human skeletal disorders such as Crouzon syndrome,[24,25] achondroplasia,[26−29] and thanatophoric dysplasia.[29−31] Therefore, discovery of inhibitors of FGFR kinases has substantial potential therapeutic value.[32,33]

Kinase inhibition can be achieved by competition with the substrate, with ATP, or by locking the kinase into an inactive state.[34,35] The human genome encodes at least 518 protein kinases.[36] All protein kinases share common sequences and structural homology in their ATP binding sites, making selectivity an issue in the development of kinase inhibitors. However, the less well conserved areas of the ATP binding site can be exploited to increase selectivity, if desired. Important classes of FGFR1 inhibitors presently known include indolinones[32] such as SU4984 (**1**) and SU5402 (**2**) in Figure 1, substituted pyrido[2,3-*d*]pyrimidines such as PD173074 (**3**),[33,37] and the closely related 3-aryl-1,6-napthyridine-2,7-diamines.[38] These compounds show varying kinase inhibitory strengths and selectivities. **1** inhibits the kinase activities of FGFR1, PDGFR, and insulin receptor (InsR), but it does not inhibit the kinase activity of EGFR.[32] **2** is more selective. It inhibits the tyrosine kinase activity of FGFR1, it is a weak inhibitor of PDGFR, and it does not inhibit the activity of InsR and EGFR.[32] **1** and **2** inhibit the activity of FGFR1 kinase with IC_{50} values of 10−20 μM.[32] However, **3** shows high selectivity for FGFR1, inhibiting its activity with nanomolar potency while inhibiting Src, InsR, EGFR, PDGFR, and several other kinases with 1000-fold or higher IC_{50} values.[33] Several FGFR kinase inhibitors, particularly in the indolinone and 1*H*-quinolin-2-one classes, are currently in clinical trials. Like the highly successful indolinone sunitinib, they are multikinase inhibitors.[39]

†PDB accession code for the crystal structure of FGFR1 kinase with **4** is 3JS2.

*To whom correspondence should be addressed. Phone: 203-432-6278. Fax: 203-432-6299. E-mail: William.Jorgensen@yale.edu.

[a] Abbreviations: ATP, adenosine triphosphate; EDTA, ethylenediaminetetraacetic acid; EGFR, epidermal growth factor receptor; FEP, free energy perturbation; FGFR, fibroblast growth factor receptor; GB/SA, generalized Born/surface area; InsR, insulin receptor; MC, Monte Carlo; MEK, mitogen-activated extracellular signal-regulated kinase; MES, 2-(*N*-morpholino)ethanesulfonic acid; OPLS-AA, optimized potentials for liquid simulations−all-atom; PDGFR, platelet-derived growth factor receptor; SP, standard precision; VEGFR, vascular endothelial growth factor receptor; XP, extra precision.

 Published on Web 02/02/2010

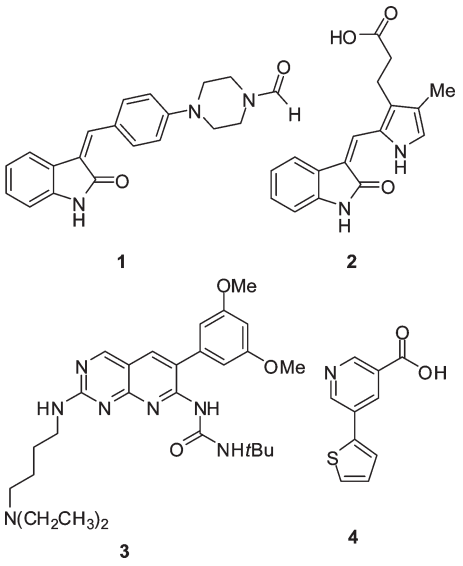

Figure 1. Examples of inhibitors of FGFR1 kinase with available crystal structures: indolinones **1** and **2**, the pyridopyrimidine **3** and **4**.

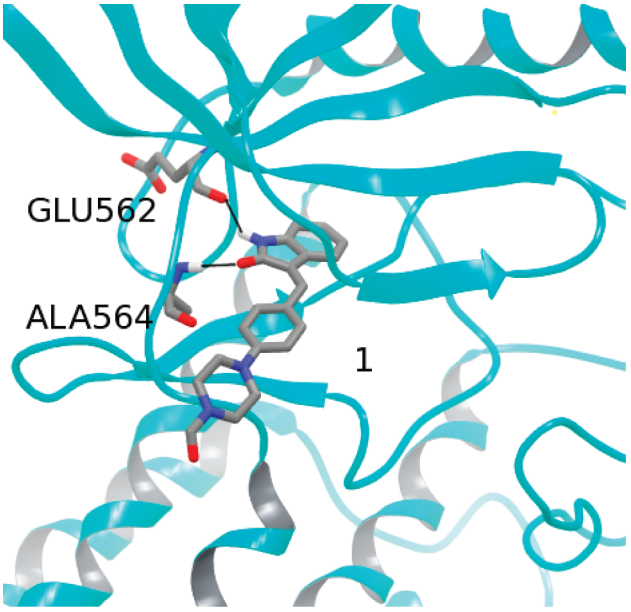

Figure 2. Indolinone **1** bound in the ATP binding site of FGFR1 kinase. Hydrogen bonds formed with Glu562 and Ala564, which are in the hinge region, are highlighted.

FGFR1 kinase consists of two subdomains enclosing the ATP binding cleft.[32,33] This cavity, which is occupied by adenine of ATP or the core of the inhibitors, is lined by hydrophobic residues. When bound, **1** forms two hydrogen bonds with the backbone carbonyl oxygen of Glu562 and nitrogen of Ala564, which belong to the hinge region connecting the two lobes (Figure 2). Crystal structures of the inhibitors **1**, **2**, and **3** bound to FGFR1 kinase[32,33] indicate that they reside in the ATP binding site and have at least one of the two hydrogen bonds with the hinge region.

The crystal structure of FGFR1 kinase bound to **1**[32] shows the nucleotide binding loop in a disordered conformation, whereas the loop is in an extended conformation in the crystal structures of FGFR1 kinase complexed with **2**[32] and **3**.[33] At the outset of the present work, we determined a crystal structure of FGFR1 kinase with the 5-thiophen-2-yl derivative of

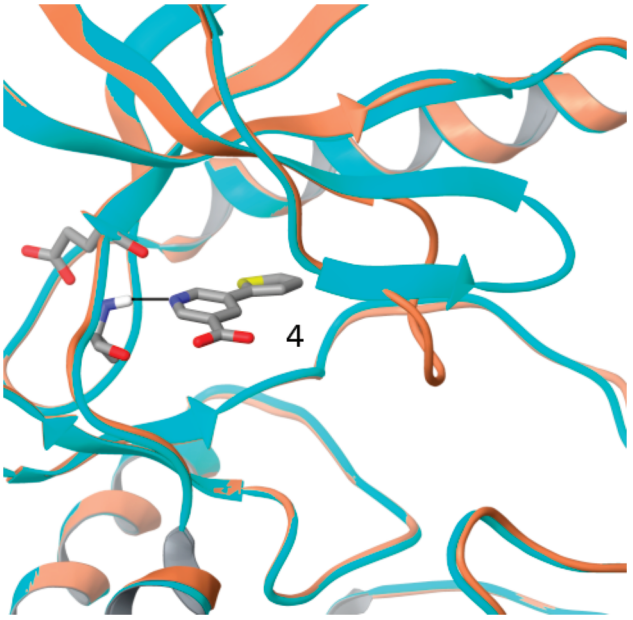

Figure 3. Crystal structures of FGFR1 kinase with **4** illustrating the two conformations for the nucleotide binding loop: extended or up (blue) and down (brown).

nicotinic acid, **4** (Figure 1), at a resolution of 2.2 Å.[40] This small inhibitor resides in the ATP binding site and forms a hydrogen bond with the nitrogen of Ala564. Notably, the crystal structure also reveals two conformations in the same crystallographic unit, one with the nucleotide binding loop down (brown in Figure 3) and the other with the loop extended, forming part of a β-strand, and pointing upward (blue in Figure 3). An issue with structure-based inhibitor design for FGFR1 kinase is, thus, the flexibility of the protein in this region.

Consequently, in view of the potential therapeutic importance and available crystallographic data, FGFR1 kinase is a compelling target for structure-based inhibitor design. However, no prospective virtual screening studies have been reported previously for discovery of FGFR kinase inhibitors. Thus, the present study was carried out (a) to seek novel leads as inhibitors of FGFR1 kinase by virtual screening and (b) to test the viability of current docking methodology for this purpose. High potency and selectivity were not expected at this stage; rather, a foundation for subsequent lead optimization was sought. The study illustrates complexities associated with the choice of protein structures for docking, possible use of multiple kinase structures to seek selectivity, practical restrictions on numbers of compounds that can be purchased and assayed, and hit identification. In particular, we have docked a large database of molecules into the ATP binding site of FGFR1 kinase using both conformations for the nucleotide binding loop in the cocrystal structure for **4**. Compound selection was also influenced by docking results for five additional kinases. Subsequent in vitro assaying followed by validation of active compounds and initial optimization did lead to the discovery of several compounds with new core structures that exhibit low-micromolar inhibition of FGFR1 kinase.

Methods

Virtual Screening. The ZINC database[41] was docked into the two conformations from the FGFR1-**4** structure[40] using Glide

4.0.[42,43] The ZINC collection contains about 2.2 million small molecules that have been filtered to be reasonable starting points for drug design and that are commercially available. The molecules are created, as appropriate, with multiple protonation and tautomeric states. The FGFR1 kinase conformations were prepared using standard Glide protocols.[42] This includes addition of hydrogens, restrained energy-minimizations of the protein structure with the OPLS-AA force field,[44] and finally setting up the Glide grids using the Protein and Ligand Preparation Module. Crystal structures of kinases with inhibitors bound in the ATP site reveal that the inhibitors form at least one hydrogen bond with backbone amide or carbonyl groups in the hinge region. Thus, imposition of pharmacophore constraints with the hinge region has been routine in docking of molecules into the ATP sites of kinases to improve the chances of success in finding active compounds.[45−47] This practice was adopted here such that any acceptable protein−ligand complex was required to have at least one hydrogen bond with Glu562 or Ala564 (Figure 2). All 2.2 million compounds were first docked and ranked using standard precision (SP) Glide.[42] The resultant top 40000 compounds were then docked using the more accurate and computationally intensive extra-precision (XP) mode.[43] The 41 compounds[48] known to exhibit activity against FGFR1 kinase including 15 indolinones such as **1** and **2**, 15 pyrido-[2,3-*d*]pyrimidines such as **3**, and 10 napthyridines, were also included. The processing of the known active compounds was intended to help gauge the effectiveness of the screening strategy. The top 1000 compounds for both conformations from the XP docking were also docked into five additional kinase structures, EGFR,[49] InsR,[50] VEGFR2,[51] Src,[52] and MEK,[53] in order to see if the current scoring is accurate enough to provide some kinase selectivity. Compounds that were eventually purchased ranked in the top 100 for FGFR1 but not in the top 100 for any of the other five kinases.

Docking with Glide effectively performs a systematic search of the conformational, orientational, and positional space for the docked ligand in the binding site of the protein. This is followed by torsionally flexible energy optimization on an OPLS-AA[44] potential energy grid to arrive at a few final candidate poses. The lowest energy poses are further refined by Monte Carlo sampling. The scoring function used in (SP) Glide includes terms for ligand−protein interaction energies, hydrophobic interactions, hydrogen bonds, internal energies, and desolvation.[42] The more sophisticated XP scoring function also employs terms that account for ligand−protein structural motifs that lead to enhanced binding affinity.[43] This includes hydrophobic enclosure, where lipophilic ligand atoms are enclosed on opposite faces by lipophilic protein atoms, and single or correlated hydrogen bonds in hydrophobic environments, which are relevant for kinase inhibitors in the ATP site. Thus, XP Glide is expected to be well suited for the study of ligand−kinase complexation.

The resultant most desirable compounds were also evaluated for conformational strain in the bound conformation. One measure of this strain is the root-mean-square deviation between a molecule's docked structure and its structure after energy minimization in vacuum. Another measure that was applied is the difference in energy after minimization and the lowest energy conformation resulting from a 200 conformation Monte Carlo search with GB/SA hydration using the program *BOSS*.[54] These measures revealed that most compounds of interest were in reasonably favorable conformations in the protein binding site. Visual inspection of poses was also essential in arriving at the final selections, which were then purchased from commercial vendors.

MC/FEP Simulations. Some Monte Carlo/free-energy perturbation calculations were executed to compute relative free energies of binding in order to guide initial modifications of active compounds. The calculations were performed following standard protocols with the program *MCPRO*.[54] The models were built starting from the crystal structure for the complex with **4** and included the 170 amino acid residues nearest the ligands. Short conjugate-gradient minimizations were carried out on the initial structures for all complexes to relieve any unfavorable contacts. Coordinates for the unbound ligands were obtained by extraction from the complexes. The unbound ligands and complexes were solvated in 25 Å caps with ca. 2000 and 1250 water molecules. The FEP calculations utilized 11 windows of simple overlap sampling. Each window covered 10−15 million (M) configurations of equilibration and 20−30 M configurations of averaging. The ligand and side chains with any atom within ca. 10 Å of the ligand were fully flexible, while the protein backbone was kept fixed during the MC simulations. The energetics were evaluated with the OPLS-AA force field for the protein, OPLS/CM1A for the ligands, and TIP4P for water.[44]

Experimental. Purchased compounds were initially assayed as received. Structures of active and new compounds were validated through ^{1}H and ^{13}C NMR and high-resolution mass spectrometry, as detailed in the Supporting Information. The purity of all active and new compounds was demonstrated to be $>95\%$ by high-performance liquid chromatography. Synthetic schemes for new compounds are provided below, while the synthetic details are provided in the Supporting Information.

Biological assaying was performed using ALPHAScreen (Amplified Luminescent Proximity Homogeneous Assay) from Perkin-Elmer. FGFR1 kinase, the biotinylated peptide, ATP, and the potential inhibitor were added to each of 10 wells with inhibitor concentrations typically ranging from 0.01 to 250 μM. Phosphorylation of the peptide was allowed to proceed for 30 min, and then the reaction was stopped by adding EDTA. The resultant differential phosphorylation of the peptide by FGFR1 kinase in each well depends on the effectiveness of the inhibitor. Acceptor beads coated with antiphosphotyrosine antibodies and donor beads coated with streptavidin conjugates are then introduced into each well. Biotinylated peptide is efficiently captured by the donor bead. The FGFR1 kinase domain was obtained and purified as previously described.[55] Other kinases used in this study, EGFR, InsR, and Src, were obtained from Millipore Corp.

Purified FGFR1 kinase domain (20 mg/mL) was cocrystallized with 2-thienyl nicotinic acid, **4** (1 mM), by vapor diffusion in 0.1 M MES-NaOH (pH 6.5), 14% PEG 4000, 0.2 M $(NH_4)_2SO_4$, and 5% glycerol at 4 °C. The crystals were flash frozen in 0.1 M MES (pH 6.5), 25% PEG 4000, 0.2 M $(NH_4)_2SO_4$, and 10% glycerol. Diffraction data were collected on beamline X29 at the National Synchrotron Light Source. They were processed by using HKL2000, and a molecular replacement solution for the complex was found by using the structure of inactive FGFR1 (PDB ID: 1FGK).[56] The resultant structure has been deposited in the Protein Data Bank (PDB ID: 3JS2).[40]

Results

Docking Known Inhibitors. The top 40000 compounds emerging from the SP Glide calculations plus the 41 compounds possessing known activity were processed with XP Glide. For both loop conformations, eight of the known active compounds ended up in the top 1000. There were four active compounds in common, and thus 12 unique active compounds were retrieved. Assuming equal distribution of the 41 compounds in 40000, there is roughly 1 in every 1000. Thus, the finding of eight in the top 1000 reflects significant enrichment. If the top 10000 compounds are considered, 17 and 11 of the known active compounds were identified using the protein conformation with the binding loop down and up, respectively. The performance of SP Glide alone can also be noted. When the 41 known active compounds are added

to the 2.2 million library compounds, 9 and 10 are ranked in the top 10000 using the protein conformations with the binding loop down and up, respectively, and 12 and 11 compounds are among the top 50000. The random result would be retrieval of roughly 1 known active compound per 50000. Thus, docking with Glide in both SP and XP modes demonstrated success in identifying known FGFR1 kinase inhibitors. Additional benefits of the XP mode over SP were not clearly apparent in this exercise. As detailed below, the performance of XP Glide for the known inhibitors was also class specific.

Superposition of the crystal structures with the poses from Glide reveals good correspondence for the positioning of **1** and **2** (Figure 4). In general, among the known active compounds, ones with the indolinone core show the correct orientation when compared to the crystal structures of the complexes for **1** and **2**.[32] There is also very good overlap of the positions of **4** in the crystal structure[40] and in the docked complexes for both conformations of the nucleotide binding loop. However, the docked structure for FGFR1 kinase with the nucleotide binding loop up complexed with **3** has incorrect orientation of the ligand (Figure 4). Superposition of structures of complexes with compounds having the pyrido-[2,3-*d*]pyrimidine or napthyridine cores from the XP docking and the crystal structure of **3** reveal a 180° flip in the binding site (Figure 4). The crystal structures used for the docking were the ones for **4**, as this was the most complete structure with no missing residues. However, most of the pyridopyrimidine inhibitors have large side chains, which clash sterically with the side chain of Lys514 when the inhibitor's core is properly oriented. Thus, incorrect docking of the pyrido-[2,3-*d*]pyrimidine class could be improved by screening against additional conformations of FGFR1 kinase. This would hopefully lead to additional compounds with very low docking scores that could be further scrutinized. Alternatively, the conformational problem argues in favor of fragment screening to discover viable core structures without the need to accommodate large substituents. Owing to these considerations, 8 of the 12 unique active compounds in the top 1000 from the XP docking with the nucleotide binding loop in either orientation belong to the indolinone class. The correct docking of these compounds presumably accompanies their good rankings. The compounds in the pyrido-[2,3-*d*]pyrimidine and the napthyridine classes are incorrectly docked and rank poorly.

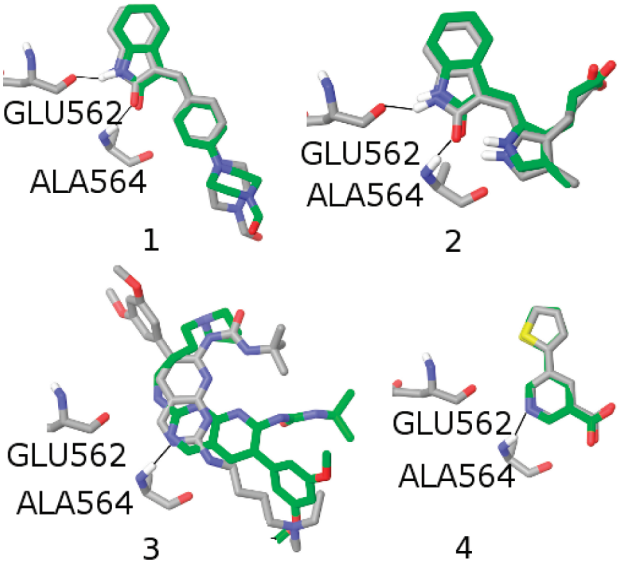

Figure 4. Overlays of the crystal structure (gray) with the XP GLIDE pose (green) for **1**, **2**, **3**, and **4**. Hydrogen bonds with Glu562 and Ala564 are highlighted.

The distribution of XP scores for the 40000 compounds from the ZINC library, when docked into either FGFR1 kinase conformer, covers a 16 kcal/mol range (Figure 5). Many library compounds have scores as low as those for the best-ranked known actives (in red in Figure 5). Although it is encouraging that many compounds from ZINC yield such favorable scores, many known active compounds have poor scores in view of the incorrect docking.

Compound Selection and Activity. The 2000 library compounds, 1000 for each FGFR1 conformer, with the best XP scores, were processed further. For both conformers, to favor compounds that could selectively inhibit FGFR1 kinase, the top 1000 compounds were docked into the ATP binding sites for the five other kinases, EGFR, InsR, VEGFR2, Src, and MEK. While the kinome has roughly 500 members,[36] this subset was chosen based on potential availability of the protein for assaying and, of course, availability of a cocrystal structure of the kinase with a ligand in the ATP site. Compounds ranked within the top 100 for FGFR1 kinase, but not in the top 100 for any of the other 5 kinases, were retained for further consideration. Their docked protein−ligand complexes received extensive visual inspection. Ligands that possessed inappropriate geometries such as twisted amides or esters were rejected.[57] The compounds were also checked for excessive conformational strain in the bound conformation, as described above.

At this point, for the set of compounds from the screening of the conformation with the binding loop up, a total of 31 desirable compounds remained. To promote structural diversity, this set was further partitioned into 14 chemical classes. Eventually, 11 compounds, which were mostly the

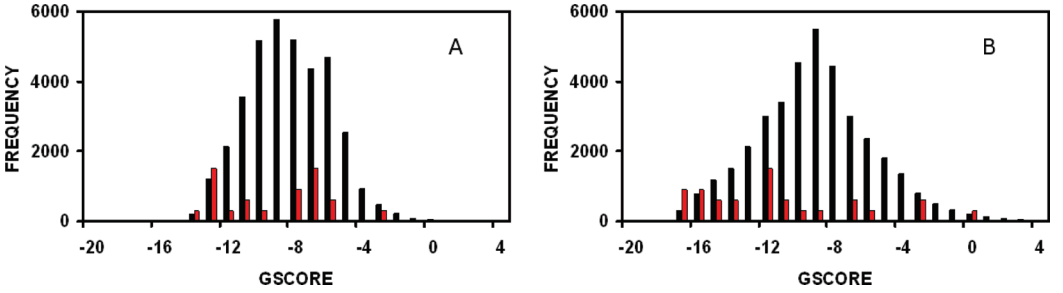

Figure 5. XP Glide score frequency for 40000 compounds from the ZINC collection in black and known active compounds in red (scaled by 300) for the conformation with (A) the nucleotide binding loop up and (B) with the nucleotide binding loop down.

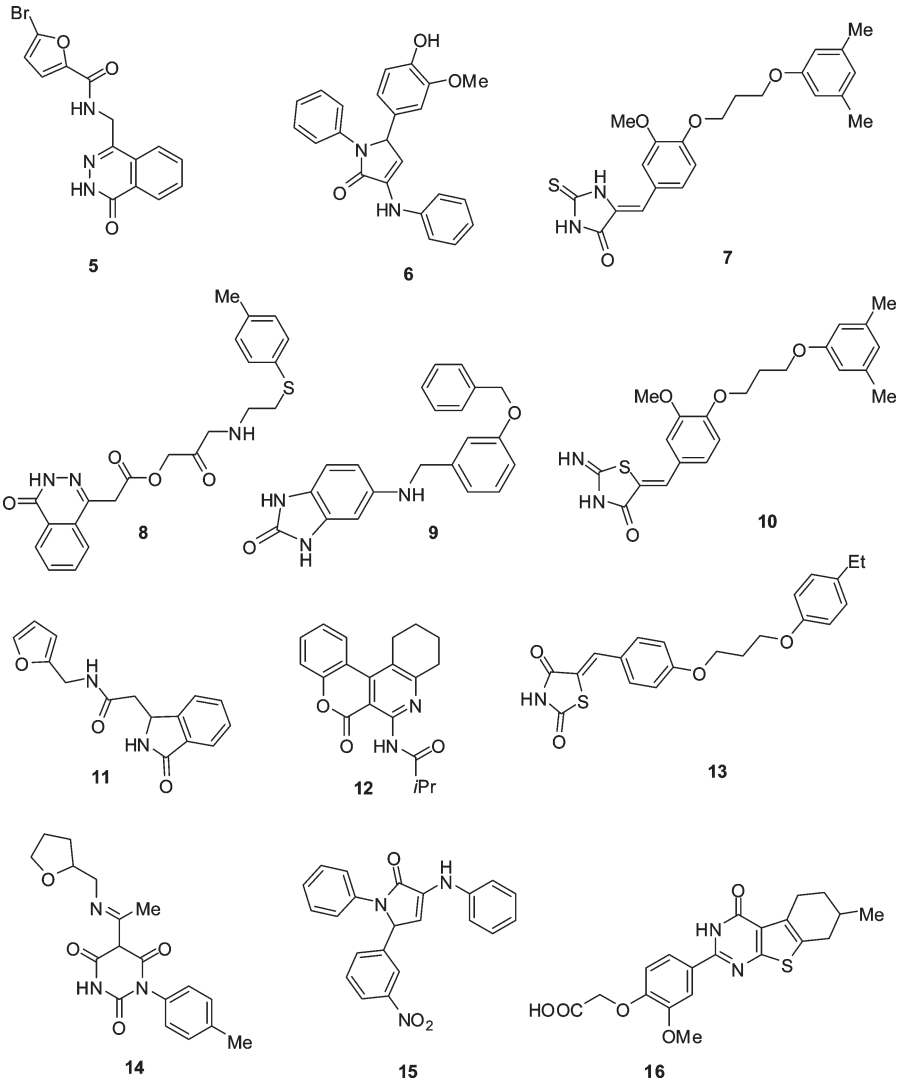

Figure 6. Structures of the purchased compounds obtained by docking into the conformation of FGFR1 kinase with the nucleotide binding loop up. Although **7** was ordered, it turned out to be the isomer **10**. Samples of both **7** and **10** were synthesized.

top-ranked in their class, were purchased. These are shown in Figure 6. In one case, **7**, structural ambiguity arose, and it was subsequently determined that the purchased compound was actually the isomer **10**. As described below, this was demonstrated through synthesis and assaying of both **7** and **10**. The docked structures and scores for **7** and **10** are essentially identical, as the structural difference is in the edge that is solvent-exposed in the complexes. Thus, the structures of the two isomers, **7** and **10**, and the 10 other purchased compounds are shown in Figure 6. This set has a good representation of five- and six-membered heterocycles including six with fused polycyclic ring systems. Not surprisingly, in the docked structures, the polycyclic cores overlap the position of adenine of ATP when bound. All computed structures of the complexes feature hydrogen bonds in the hinge region and extensive overlap with the positions of known inhibitors in crystal structures for complexes with FGFR1 kinase.

In the same manner, the top 1000 compounds from the docking calculations with the FGFR1 binding loop in the down conformation were narrowed to 37 compounds, which were assigned to 15 classes. Among these, the 12 high-ranking ones in Figure 7 were ultimately purchased. In both cases, compounds with cores not previously reported as FGFR1 kinase inhibitors were sought; indolinones, naphthyridines, and compounds with 2-aminopyrinidine fragments were avoided. A total of 23 compounds was purchased and tested in vitro for inhibition of FGFR1 kinase using the AlphaScreen assaying system. The results of the assaying along with Glide scores and ranks are shown in Table 1. Two of the compounds were found to inhibit the activity of FGFR1 kinase. Although follow-up of these hits is enough to consume our available resources, purchase and assaying of at least all 68 of the compounds deemed most desirable would likely have generated additional alternatives. It is also expected that many of the core structures for the inactive compounds among **5**−**28**, in fact, provide viable platforms for discovery of active inhibitors; small changes are often all that is needed to turn an inactive compound into an active one.[58,59]

7, 10, and Analogues. One of the purchased compounds from ChemBridge Corp., presumed to be **7**, had an IC_{50} value of 23 μM. For initial follow-up, **7** and several analogues, **29**−**34**, were synthesized as summarized in Scheme 1. The intention was exploration of modifications to the methoxy group in **7** and a chlorine scan for the terminal phenyl ring. MC/FEP results indicated that chlorine and methyl substitution should be most favorable at the meta positions

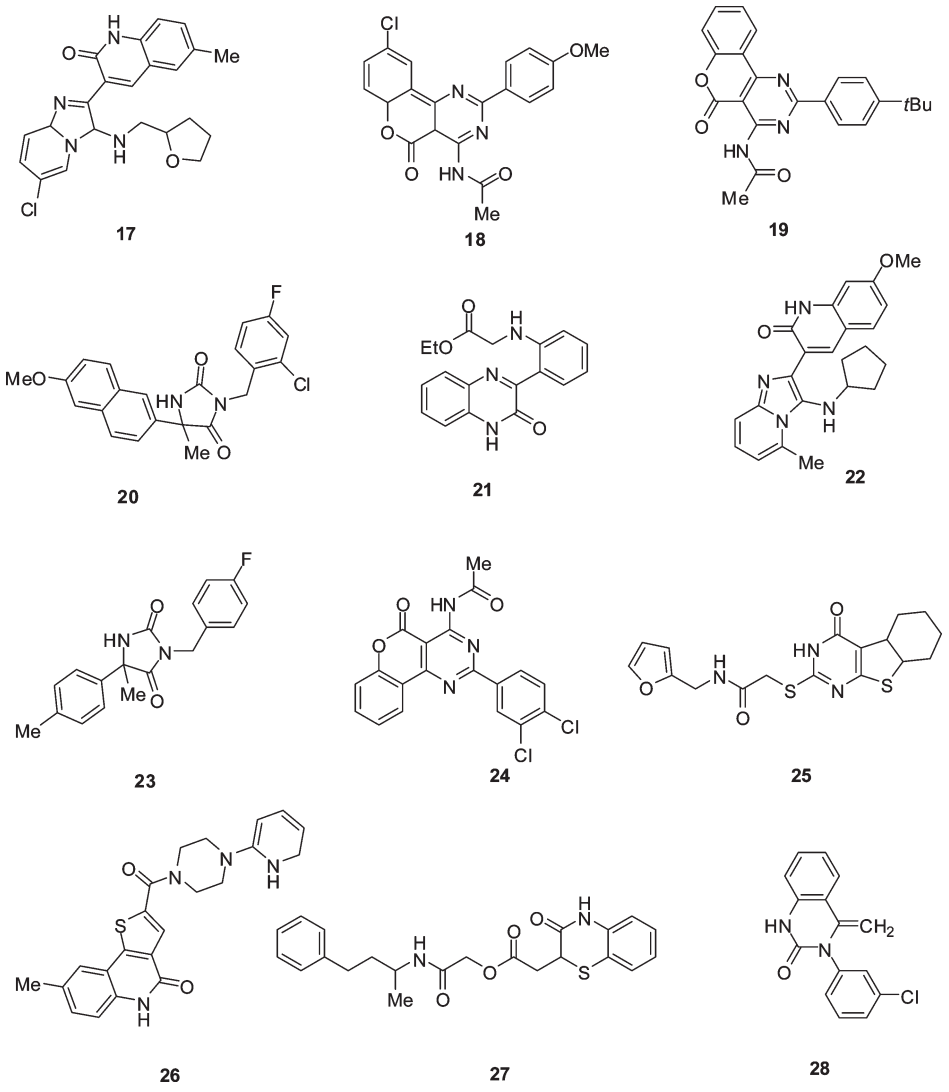

Figure 7. Structures of the purchased compounds obtained by docking into the conformation of FGFR1 kinase with the nucleotide binding loop down. Compounds with stereocenters are racemic mixtures.

in this ring. The benzylidene derivatives were prepared from either commercially available *p*-hydroxybenzaldehyde or 3-alkoxy-4-hydroxybenzaldehydes. In the case of **29**, first *p*-hydroxybenzaldehyde (**41**) was converted to 3- methoxymethyl-4- hydroxybenzaldehyde (**42c**). The aldehydes **43a**−**c** resulted from *O*-alkylation of **42a**−**c** with 1,3-dibrompropane. The *O*-alkylation of alkyl bromides **43a**−**c** with phenols **44a**−**d** then provided aldehydes **45a**−**g**, and Knoevenagel condensation of **45a**−**g** with thiohydantoin afforded **7** and **29**−**34**.

The compounds were assayed (Table 2), and it was surprising to find that **7** was now inactive and that only **29** and **30** showed weak activity. A small molecule crystal structure was then obtained for **31**, which confirmed the structures in this series to be as shown in Table 2, notably with the thiohydantoin substructure and *Z*-olefin geometry. Thus, the purchased compound displaying the 23 μM activity was not **7**. Scrutiny of the NMR spectra for the purchased compound and the synthesized **7** led to the expectation that the purchased compound might be the pseudothiohydantoin isomer **10**. This compound was then prepared by Knoevenagel condensation of aldehyde **45a** with pseudothiohydantoin (Scheme 1). The AlphaScreen assay demonstrated that **10** was the active compound (Table 1), and the spectral data confirmed that **10** and the purchased compound were the same. Compound **10** was subsequently docked into FGFR1 kinase. The predicted pose is almost identical to that for **7**, and it was found to rank well (Table 1). **10** also showed poor ranking against the other 5 kinases, thus meeting the computational selectivity criterion. In summary, extensive validation was needed to confirm that **10** rather than **7** was the active compound found in the screening.

16 and Analogues. Thienopyrimidinone **16** is the other purchased compound that was found to inhibit the activity of FGFR1 kinase. However, the IC_{50} value of 50 μM was modest, so some initial lead optimization was pursued to see if a simple analogue in the low μM range could be obtained. To examine the role of the carboxylic acid side chain of **16**, which was predicted to be largely solvent exposed in the complex with FGFR1 kinase, compounds **35** and **36** were synthesized, as shown in Scheme 2. Relatives with the tricyclic core fully unsaturated such as **37**−**40** were also pursued. MC/FEP calculations were performed and indicated that replacement of H by methyl at R_1 and R_2 should improve the free energy of binding by 2.2−2.6 kcal/mol. Introduction of a methyl group at the open position adjacent

to R_1 was computed to be a little less favorable, while a methyl group at the remaining site adjacent to R_2 is highly unfavorable owing to steric clashes with the backbone of Glu562. Finally, given the experience with **7** and **10**, **16** too was synthesized.

Preparation of thiouracil derivatives **16** and **35**−**40** commenced with 3- or 4-substituted cyclohexanones. Gewald reaction of cyclohexanones **46a**−**e** with 2-cyanoacetamide provided 2-aminothiophenes **48a**−**e**. Condensation of **48a** with aldehyde **52** provided ester **49**, which was hydrolyzed to afford **16**. The spectra for the purchased **16** and synthesized **16** were the same. The reaction of 2- aminothiophene **48a** with 3,4-dimethoxybenzaldehyde and 3-methoxybenzaldehyde resulted in the formation of **35** and **36**. For the synthesis of benzothiophene derivatives **37**−**40**, first, the 2-aminothiophenes **48a**−**e** were converted to 2-aminobenzothiophenes 50a−**e**. Acid-catalyzed condensation of **50a**−**e** with aldehyde 52 resulted in esters **51a**−**e**, which were hydrolyzed to yield 37−**40**.

As summarized in Table 3, the decarboxylated **35** and **36** do not inhibit FGFR1 kinase. However, the unsaturated analogues, **37** and **40**, provided significant advance (Table 4). Conversion of the cyclohexyl ring to phenyl in going from **16** to **37** lowered the IC_{50} from 50 to 4 μM. This outcome was not obvious owing to the trade-off between greater hydrophobicity with **16** and greater rigidity with **37**. Replacing the methyl substituent by ethyl in proceeding from **37** to **38** yielded little change in activity, while introduction of trifluoromethyl at R_1 in **39** eliminated activity. Consistent with the MC/FEP results, a methyl group was found to have similar effect at R_1 and R_2, with **40** being the most active analogue with an IC_{50} of 1.9 μM. Overall, the unsaturated analogues **37**, **38**, and **40** provide a novel core structure for FGFR1 kinase inhibition and a much improved starting point for full lead optimization.

Table 1. Experimental IC_{50} Values for Inhibition of FGFR1 Kinase and Glide Scores and Rankings

compd	XP rank	XP score	SP rank	IC_{50} (μM)[a]
5	1	−16.18	112	na
6	7	−14.84	11628	na
7	16	−14.29	33929	na
8	19	−14.20	22167	na
9	25	−13.98	550	na
10	38	−13.79	61627	23
11	46	−13.71	8409	na
12	51	−13.66	13883	na
13	52	−13.64	6377	na
14	74	−13.49	36663	na
15	77	−13.48	396	na
16	84	−13.45	20052	50
17	2	−18.53	429	na
18	10	−17.38	10443	na
19	29	−17.01	12782	na
20	37	−16.96	7676	na
21	41	−16.93	14137	na
22	45	−16.89	19473	na
23	55	−16.84	9711	na
24	56	−16.84	15905	na
25	64	−16.78	6525	na
26	72	−16.75	4238	na
27	93	−16.62	27217	na
28	97	−16.60	22135	na

[a] na indicates not active in the assay.

Table 2. Experimental IC_{50} Values for Inhibition of FGFR1 Kinase by Analogues of **7**

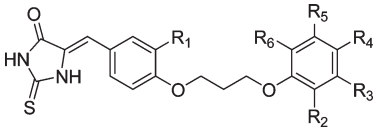

compd	R_1	R_2	R_3	R_4	R_5	IC_{50} (μM)
7	OMe		Me		Me	na
29	OEt		Me		Me	250
30	CH_2OMe		Me		Me	3300
31	OMe	Cl				na
32	OMe		Cl			na
33	OMe			Cl		na
34	OMe		Me			na

Scheme 1[a]

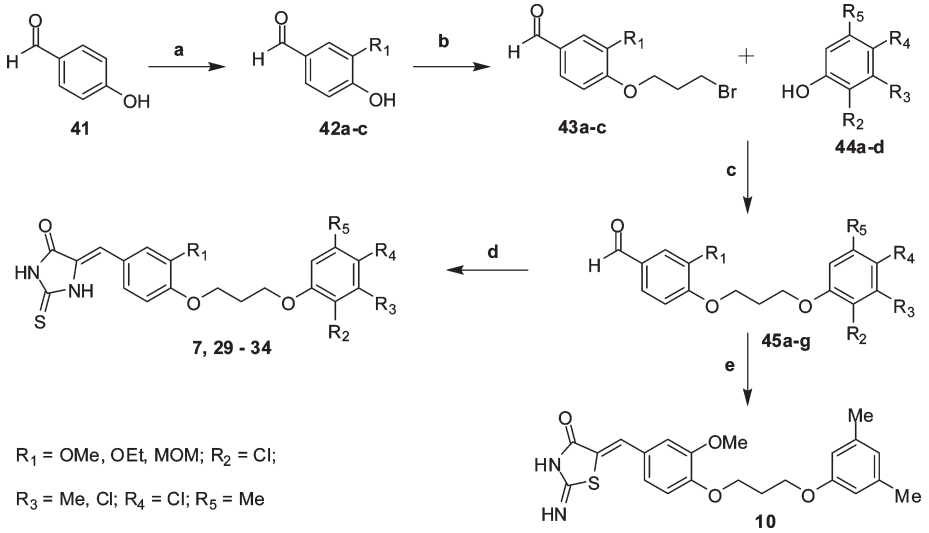

[a] Reagents and conditions: (a) (1) HCHO, HCl, 50 °C, 3 h; (2) MeOH, reflux, 3 h, 57% two steps. (b) 1,3-Dibromopropane, K_2CO_3, DMF, 80 °C, 1 h (43−60%). (c) K_2CO_3, DMF, 80 °C, 1 h (44−91%). (d) Thiohydantoin, pipiridine, MeOH, reflux (54−74%). (e) pseudothiohydantoin, AcONa, AcOH, 170 °C, 15 min, MW, 53%.

Scheme 2[a]

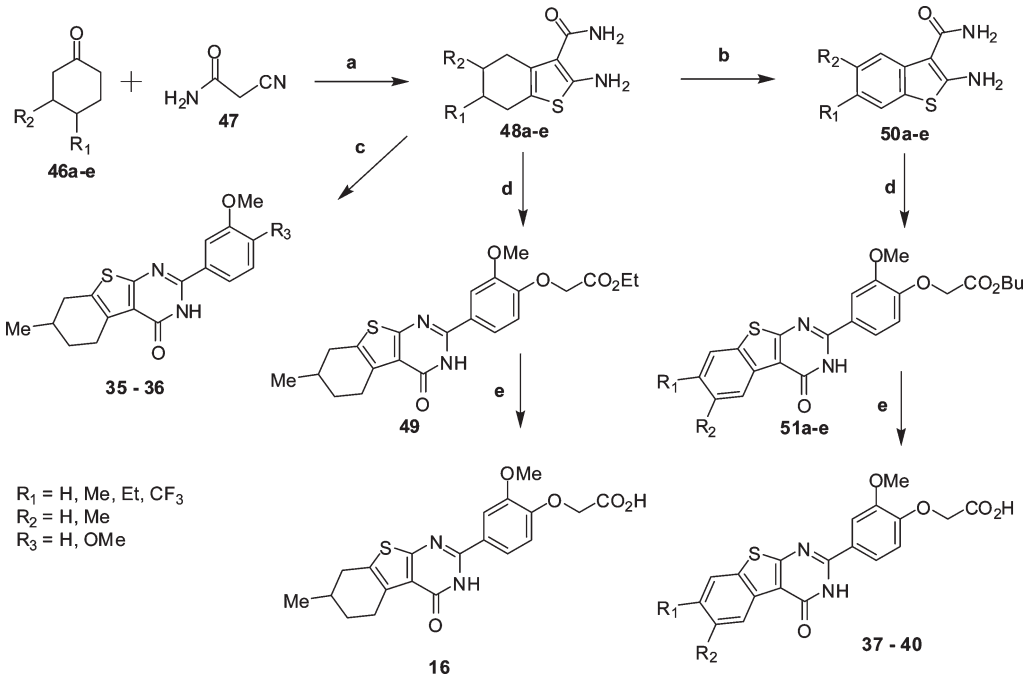

[a] Reagents and conditions: (a) S, piperidine, EtOH, 50 °C, 4 h (23−60%); (b) *p*-chloranil, 1,4-dioxane, 90 °C, 5 h; (c) 3,4-dimethoxybenzaldehyde or 3-methoxybenzaldehyde, conc HCl, *n*-BuOH, 80 °C, 8H (48−67%); (d) ethyl 2-(4-formyl-2-methoxyphenoxy)acetate (**52**), conc HCl, *n*-BuOH, reflux, 2 h (30−62%); (e) 5N NaOH, EtOH, reflux, 2 h (30%-quant).

Table 3. Inhibitory Activities of FGFR1 Kinase by Analogues of **16**

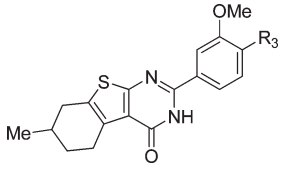

compd	R_3	IC_{50} (μM)
16	OCH_2CO_2H	50
35	OMe	na
36	H	na

Table 4. Inhibitory Activities of FGFR1 Kinase by Tetradehydro Analogues of **16**

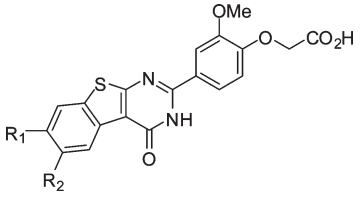

compd	R_1	R_2	IC_{50} (μM)
37	Me	H	4.0
38	Et	H	5.5
39	CF_3	H	na
40	H	Me	1.9

Computed Properties, Structures, and Selectivity for 10 and 40. Thus, the screening and subsequent synthetic efforts delivered two principal compounds, which are suitable for further lead optimization, the pseudothiohydantoin derivative **10** with an IC_{50} of 23 μM and the benzothienopyrimidinone derivative **40** with an IC_{50} of 1.9 μM. To our knowledge, no compounds with these core structures have been demonstrated previously to be FGFR1 kinase inhibitors. Both compounds evolved from the docking calculations that used the conformation of FGFR1 kinase with the nucleotide binding loop in the extended conformation (Figure 3). The chosen compounds that came from the docking calculations with the nucleotide binding loop down (Figure 7) were all inactive. This should not be overinterpreted in view of the modest success in finding only one true active compound, **16**, among the 23 compounds, which were purchased. More favorable XP scores were obtained for the conformation with the binding loop down (Table 1); however, a possible reorganization penalty for achieving this conformation is not included in the calculations.

Table 5. Some Properties of the Lead Compounds Predicted Using *QikProp* 3.0

compd	MW[a]	QP log P[b]	QP log S[c]	QP PCaco2[d]	N metabolites[e]
10	412.5	4.49	−6.1	673	6
40	396.4	3.26	−5.6	36	5

[a] Molecular weight. [b] Log of the octanol/water partition coefficient. [c] Log of the aqueous solubility S (mol/L). [d] Caco2 cell permeability in nm/s. [e] Number of primary metabolites.

To provide an initial sense of expected pharmacological properties, the program *QikProp*[60] was used to make the predictions in Table 5. The selected properties are expected to influence bioavailability through dissolution, cell permeation, and metabolism. When *QikProp* is run for a set of 1700 oral drugs, 95% are predicted to have molecular weights between 130 and 500, log P values between −2 and 6, log S values between −6.0 and 0.5, PCaco2 values greater than 25 nm/s, and seven or fewer primary metabolites.[61] The predicted properties of the two key compounds compare

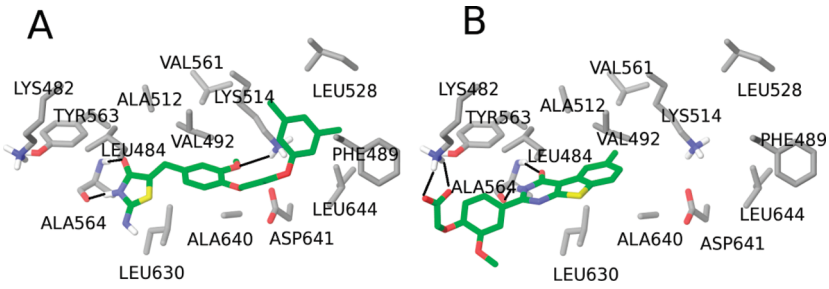

Figure 8. Computed structures for the complexes of FGFR1 kinase with **10** (A) and **40** (B). Selected backbone and side-chain atoms of the kinase are shown; carbon atoms of the inhibitors are colored green. Hydrogen bonds are highlighted with black lines.

favorably with these ranges, although poorer solubility needs to be avoided during further lead optimization. For **10**, the predicted primary metabolites arise from ether cleavages, benzylic methyl oxidations, and possible sulfur oxidation. For **40**, the predicted metabolic processes are for oxidation of the sulfur atom and the three side chains leading to possible catechol formation.

The structures from the Glide XP docking for **10** and **40** are illustrated in Figure 8. Both ligands are predicted to bind in the hinge region and both feature two hydrogen bonds with Ala564 via the amido fragments (O=C-NH) in the pseudothiohydantoin and pyrimidinone rings. There is considerable overlap with the observed positioning of the indolinones, e.g., in Figure 2.[32] However, the hydrogen-bonding motif is interestingly different because, for the indolinones, the order of the amido fragments (HN-C=O) is reversed and the complementarity is with the backbone carbonyl oxygen of Glu562 and the NH of Ala564. The bound **10** also extends more to the right toward Phe489 than for the indolinones. In addition, the complex for **10** has a hydrogen bond between the methoxy group on the ligand's central ring and the side-chain ammonium group of Lys514. The assay results for **29** in Table 2 indicate that the methoxy to ethoxy change is beneficial for binding, perhaps owing to favorable additional hydrophobic interactions in the Val492−Lys514 area, while change to methoxymethyl (**30**) is less productive. Another notable motif is the sandwiching of the dimethylphenyl ring of **10** between the side chains of Phe489 and Lys514, forming presumably constructive $\pi-\pi$ and cation$-\pi$ interactions. This does impose conformational restrictions on the 1,3-dioxypropyl linker. Returning to the **7** versus **10** conundrum, the computed structures do not provide an obvious reason for the inactivity of **7** because the S=C-NH and HN=C−S edges are predicted to be solvent exposed. Presumably, there is sensitivity of the critical hydrogen bonding with Ala564 to the geometrical and electronic differences between the isomeric rings or there are subtleties in their hydration; further computational investigation is warranted.

For **40**, additional hydrogen bonding is indicated via salt bridge formation between the ligand's carboxylate group and the ammonium terminus of Lys482. These groups can also be fully solvent exposed. Thus, the energetic benefit of the salt bridge is not clear; however, the results in Table 3 indicate that the carboxylate group is making a positive contribution to the activity. The beneficial methyl groups at R_1 and R_2 in **37**, **38**, and **40** (Table 4) are inserted into the hydrophobic region near Val492. Comparison of the computed structures for the complexes of **10** and **40** suggests that lead optimization for **40** has opportunities in expansion toward Lys514 and Phe489 and truncation at the other end of the inhibitor.

Table 6. Inhibitory Activities for Four Kinases

	IC_{50} (μM)			
compd	FGFR1	EGFR	Src	InsR
10	23	56	10	47
40	1.9	2.4	1.9	na

Finally, testing of compounds **10** and **40** for activity against other kinases was performed using EGFR, InsR, and Src (Table 6). Compound **10** is an inhibitor of all four kinases with IC_{50} values of 10−56 μM, while **40** does not inhibit InsR, but it is a 2 μM inhibitor for FGFR1, EGFR, and Src. Thus, the limited computational selectivity filter was not effective; however, fundamentally, the diverse results in Figure 5 for known inhibitors of FGFR1 kinase need to be noted along with the fact that the two active compounds from the present screening had essentially the two worst scores in Table 1. Under the circumstances, the current docking and scoring methodology does not appear to be accurate enough to guide economically viable compound acquisition in the absence of substantial human postprocessing.[62] It seems even less likely that the current methodology is accurate enough to successfully address kinase selectivity, which requires reliability of the results for multiple targets. The issue is complicated by the recognition of potential clinical benefits for compounds with multikinase activity.[39] Nevertheless, there is clear value in the docking, as it did provide a key component of a compound selection protocol that enabled the discovery of two new series of FGFR1 kinase inhibitors. Selectivity is typically expected to be addressed during lead optimization through combination of more computational modeling, synthesis, assaying, and crystallography.[59]

Conclusions

The ZINC database of 2.2 million compounds was screened using two conformations of FGFR1 kinase. On docking with XP Glide, 8 of 41 known active compounds emerged in the top 1000 of 40000 compounds, which were the best ranked ones using SP Glide. The indolinone class of inhibitors and nicotinic acid derivative **4** were handled well, while the docked structures and scoring for the pyrido[2,3-*d*]pyrimidine and napthyridine classes were inaccurate. The conformation of Lys514 in the utilized structure led to steric incompatibilities with many of the known inhibitors. The virtual screening progressed to the purchase of 23 structurally diverse compounds. Two compounds were initially found to be active. However, much effort was needed to demonstrate that the structure for one was incorrectly assigned and that the isomer

10 was the true active compound; synthesis of both isomers was required. **10**, a benzylidene derivative of pseudothiohydantoin, and **16**, a thienopyrimidinone derivative, were found to show inhibitory activity toward FGFR1 kinase with IC_{50} values of 23 and 50 μM. Modifications of **16** led to the more unsaturated **40**, which showed a much improved IC_{50} value of 1.9 μM. The predicted structures for the complexes of FGFR1 kinase with **10** and **40** appear reasonable in comparison to known crystal structures, and they are generally consistent with the initial structure−activity results presented here. Both compounds are expected to form two hydrogen bonds with the oxygen and amide NH of Ala564; aryl−aryl, cation−π, and salt bridge interactions are also represented. Finally, the selectivity of **10** and **40** for FGFR1 kinase received some analysis through assaying with three additional kinases, EGFR, InsR, and Src. Little selectivity was found, except that **40** shows no inhibition of InsR kinase. Although the applied computational selectivity filter could be made more restrictive, it is unlikely that the accuracy of the current docking and scoring methodology is sufficient to provide a solid basis for this purpose. Optimization of the two new series of FGFR1 kinase inhibitors for both potency and selectivity is being pursued using a combined approach featuring free-energy perturbation calculations, organic synthesis, biological assaying, and protein crystallography.

Acknowledgment. Gratitude is expressed to the National Institutes of Health (GM032136, AR051448, AR051886, P50-AR054086) and to Yale University (YSM0061AM) for support. The authors are also grateful to Drs. Sunilkumar Gandavadi, Christopher D. Incarvito, and Julian Tirado-Rives for spectral, crystallographic, and computational assistance.

Supporting Information Available: Synthetic details and spectral data for compounds **7**, **10**, **16**, and **29**−**40**. This material is available free of charge via the Internet at http://pubs.acs.org.

References

(1) Bishop, J. M. The molecular genetics of cancer. *Science* **1987**, *235*, 305–311.
(2) Ullrich, A.; Schlessinger, J. Signal transduction by receptors with tyrosine kinase activity. *Cell* **1990**, *61*, 203–212.
(3) Aaronson, A. S. Growth factors and cancer. *Science* **1991**, *254*, 1146–1153.
(4) Jaye, M.; Schlessinger, J.; Dionne, C. Fibroblast growth factor receptor tyrosine kinases: molecular analysis and signal transduction. *Biochim. Biophys. Acta* **1992**, *1135*, 185–199.
(5) Basilico, C.; Moscatelli, D. The Fgf Family of Growth Factors and Oncogenes. *Adv. Cancer Res.* **1992**, *59*, 115–165.
(6) Schlessinger, J. Cell Signaling by Receptor Tyrosine Kinases. *Cell* **2000**, *103*, 211–225.
(7) Klagsbrun, M.; Edelman, E. R. Biological and biochemical properties of fibroblast growth factors. Implications for the pathogenesis of atherosclerosis. *Arteriosclerosis* **1989**, *9*, 269–278.
(8) Brem, H.; Klagsbrun, M. *Oncogenes and Tumor Suppressor Genes*. In *Human Malignancies*; Benz, C. C., Liu, E. T., Eds.; Kluwer Academic: Boston, 1993; pp 211−231.
(9) Klagsbrun, M.; D'Amore, P. A. Regulators of Angiogenesis. *Annu. Rev. Physiol.* **1991**, *53*, 217–239.
(10) Adnane, J.; Gaudray, P.; Dionne, C. A.; Crumley, G.; Jaye, M.; Schlessinger, J.; Jeanteur, P.; Birnbaum, D.; Theillet, C. BEK and FLG, two receptors to members of the FGF family, are amplified in subsets of human breast cancers. *Oncogene* **1991**, *6*, 659–663.
(11) Penault-Llorca, F.; Bertucci, F.; Adélaïde, J.; Parc, P.; Coulier, F.; Jacquemier, J.; Birnbaum, D.; Delapeyrière, O. Expression of fgf and fgf receptor genes in human breast cancer. *Int. J. Cancer* **1995**, *61*, 170–176.
(12) Jacquemier, J.; Adelaide, J.; Parc, P.; Penault-Llorca, F.; Planche, J.; Delapeyriere, O.; Birnbaum, D. Expression of the FGFR1 gene in human breast-carcinoma cells. *Int. J. Cancer* **1994**, *59*, 373–378.
(13) McLeskey, S. W.; Ding, I. Y.; Lippman, M. E.; Kern, F. G. MDA-MB-134 breast carcinoma cells overexpress fibroblast growth factor (FGF) receptors and are growth-inhibited by FGF ligands. *Cancer Res.* **1994**, *54*, 523–530.
(14) Luqmani, Y. A.; Mortimer, C.; Yiangou, C.; Johnston, C. L.; Bansal, G. S.; Sinnett, D. S.; Law, M.; Coombes, R. C. Expression of 2 variant forms of fibroblast growth factor receptor 1 in human breast. *Int. J. Cancer* **1995**, *64*, 274–279.
(15) Jaakkola, S.; Salmikangas, P.; Nylund, S.; Partanen, J.; Armstrong, E.; Pyrhönen, S.; Lehtovirta, P.; Nevanlinna, H. Amplification of FGFR4 gene in human breast and gynecological cancers. *Int. J. Cancer* **1993**, *54*, 378–82.
(16) Leung, H. Y.; Gullick, W. J.; Lemoine, N. R. Expression and functional activity of fibroblast growth factors and their receptors in human pancreatic cancer. *Int. J. Cancer* **1994**, *59*, 667–675.
(17) Yamaguchi, F.; Saya, H.; Bruner, J. M.; Morrison, R. S. Differential expression of two fibroblast growth factor-receptor genes is associated with malignant progression in human astrocytomas. *Proc. Natl. Acad. Sci. U.S.A.* **1994**, *91*, 484–488.
(18) Morrison, R. S.; Yamaguchi, F.; Saya, H.; Bruner, J. M.; Yahanda, A. M.; Donehower, L. A.; Berger, M. Basic fibroblast growth factor and fibroblast growth factor receptor I are implicated in the growth of human astrocytomas. *J. Neuro-Oncol.* **1994**, *18*, 207–216.
(19) Myoken, Y.; Myoken, Y.; Okamoto, T.; Kan, M.; McKeehan, W. L.; Sato, J. D.; Takada, K. Expression of fibroblast growth factor-1 (FGF-1), FGF-2 and FGF receptor-1 in a human salivary-gland adenocarcinoma cell line: evidence of autocrine growth. *Int. J. Cancer* **1996**, *65*, 650–657.
(20) Li, J. J.; Huang, Y. Q.; Moscatelli, D.; Nicolaides, A.; Zhang, W. C.; Friedman-Kien, A. E. Expression of fibroblast growth factors and their receptors in acquired immunodeficiency syndrome-associated Kaposi sarcoma tissue and derived cells. *Cancer* **1993**, *72*, 2253–2259.
(21) Theillet, C.; Adelaide, J.; Louason, G.; Bonnet-Dorion, F.; Jacquemier, J.; Adnane, J.; Longy, M.; Katsaros, D.; Sismondi, P.; Gaudray, P.; Birnbaum, D. FGFRI and PLAT genes and DNA amplification at 8p 12 in breast and ovarian cancers. *Genes Chromosomes Cancer* **1993**, *7*, 219–226.
(22) Story, M. T. Regulation of prostate growth by fibroblast growth factors. *World J. Urol.* **1995**, *13*, 297–305.
(23) Ware, J. L. Growth factors and their receptors as determinants in the proliferation and metastasis of human prostate cancer. *Cancer Metastasis Rev.* **1993**, *12*, 287–301.
(24) Reardon, W.; Winter, R. M.; Rutland, P.; Pulleyn, L. J.; Jones, B. M.; Malcolm, S. Mutations in the fibroblast growth factor receptor 2 gene cause Crouzon syndrome. *Nat. Genet.* **1992**, *8*, 98–103.
(25) Neilson, K. M.; Friesel, R. E. Constitutive Activation of Fibroblast Growth Factor Receptor-2 by a Point Mutation Associated with Crouzon Syndrome. *J. Biol. Chem.* **1995**, *270*, 26037–26040.
(26) Shiang, R.; Thompson, L. M.; Zhu, Y. Z.; Church, D. M.; Fielder, T. J.; Bocian, M.; Winokur, S. T.; Wasmuth, J. J. Mutations in the transmembrane domain of FGFR3 cause the most common genetic form of dwarfism, achondroplasia. *Cell* **1994**, *78*, 335–342.
(27) Rousseau, F.; Bonaventure, J.; Legeai-Mallet, L.; Pelet, A.; Rozet, J.; Maroteaux, P.; Le Merrer, M.; Munnich, A. Mutations in the gene encoding fibroblast growth factor receptor-3 in achondroplasia. *Nature* **1994**, *371*, 252–254.
(28) Webster, M. K.; Donoghue, D. J. Constitutive activation of fibroblast growth factor receptor 3 by the transmembrane domain point mutation found in achondroplasia. *EMBO J.* **1996**, *15*, 520–527.
(29) Naski, M. C.; Wang, Q.; Xu, J.; Ornitz, D. M. Graded activation of fibroblast growth factor receptor 3 by mutations causing achondroplasia and thanatophoric dysplasia. *Nat. Genet.* **1996**, *13*, 233–237.
(30) Tavormina, P. L.; Shiang, R.; Thompson, L. M.; Zhu, Y. Z.; Wilkin, D. J.; Lachman, R. S.; Wilcox, W. R.; Rimoin, D. L.; Cohn, D. H.; Wasmuth, J. J. Thanatophoric dysplasia (types I and II) caused by distinct mutations in fibroblast growth factor receptor 3. *Nat. Genet.* **1995**, *9*, 321–328.
(31) Webster, M. K.; D'Avis, P. Y.; Robertson, S. C.; Donoghue, D. J. Profound ligand-independent kinase activation of fibroblast growth factor receptor 3 by the activation loop mutation responsible for a lethal skeletal dysplasia, thanatophoric dysplasia type II. *Mol. Cell. Biol.* **1996**, *16*, 4081–4087.
(32) Mohammadi, M.; McMahon, G.; Sun, Li; Tang, C.; Hirth, P.; Yeh, B. K.; Hubbard, S. R.; Schlessinger, J. Structures of the Tyrosine Kinase Domain of Fibroblast Growth Factor Receptor in Complex with Inhibitors. *Science* **1997**, *276*, 955–960.
(33) Mohammadi, M.; Froum, S.; Hamby, J. M.; Schroeder, M. C.; Panek, R. L.; Lu, G. H.; Eliseenkova, A. V.; Green, D.; Schlessinger, J.; Hubbard, S. R. Crystal structure of an angiogenesis inhibitor

bound to the FGF receptor tyrosine kinase domain. *EMBO J.* **1998**, *17*, 5896–5904.
(34) Noble, M. E. M.; Endicott, J. A.; Johnson, L. N. Protein Kinase Inhibitors: Insights into Drug Design from Structure. *Science* **2004**, *303*, 1800–1805.
(35) Liao, J. J.-L. Molecular Recognition of Protein Kinase Binding Pockets for Design of Potent and Selective Kinase Inhibitors. *J. Med. Chem.* **2007**, *50*, 409–424.
(36) Manning, G.; Whyte, D. B.; Martinez, R.; Hunter, T.; Sudarsanam, S. The Protein Kinase Complement of the Human Genome. *Science* **2002**, *298*, 1912–1934.
(37) (a) Hamby, J. M.; Connolly, C. J. C.; Schroeder, M. C.; Winters, R. T.; Showalter, H. D. H.; Panek, R. L.; Major, T. C.; Olsewski, B.; Ryan, M. J.; Dahring, T.; Lu, G. H.; Keiser, J.; Amar, A.; Shen, C.; Kraker, A. J.; Slintak, V.; Nelson, J. M.; Fry, D. W.; Bradford, L.; Hallak, H.; Doherty, A. M. Structure−Activity Relationships for a Novel Series of Pyrido[2,3-*d*]pyrimidine Tyrosine Kinase Inhibitors. *J. Med. Chem.* **1997**, *40*, 2296–2303. (b) Trumpp-Kallmeyer, S.; Rubin, J. R.; Humblet, C.; Hamby, J. M.; Showalter, H. D. Development of a Binding Model to Protein Tyrosine Kinases for Substituted Pyrido-[2,3-d]pyrimidine Inhibitors. *J. Med. Chem.* **1998**, *41*, 1752–1763.
(38) Thompson, A. M.; Connolly, C. J. C.; Hamby, J. M.; Boushelle, S.; Hartl, B. G.; Amar, A. M.; Kraker, A. J.; Driscoll, D. L.; Steinkampf, R. W.; Patmore, S. J.; Vincent, P. W.; Roberts, B. J.; Elliott, W. L.; Klohs, W.; Leopold, W. R.; Showalter, H. D. H; Denny, W. A. 3-(3,5-Dimethoxyphenyl)-1,6-naphthyridine-2,7-diamines and Related 2-Urea Derivatives Are Potent and Selective Inhibitors of the FGF Receptor-1 Tyrosine Kinase. *J. Med. Chem.* **2000**, *43*, 4200–4211.
(39) (a) Karaman, M. W.; Herrgard, S.; Treiber, D. K.; Gallant, P.; Atteridge, C. E.; Campbell, B. T.; Chan, K. W.; Ciceri, P.; Davis, M. I.; Edeen, P. T.; Faraoni, R.; Floyd, M.; Hunt, J. P.; Lockhart, D. J.; Milanov, Z. V.; Morrison, M. J.; Pallares, G.; Patel, H. K.; Pritchard, S.; Wodicka, L. M.; Zarrinkar, P. P. A quantitative analysis of kinase inhibitor selectivity. *Nat. Biotechnol.* **2008**, *26*, 127–132. (b) Kumar, R.; Crouthamel, M.-C.; Rominger, D. H.; Gontarek, R. R.; Tummino, P. J.; Levin, R. A.; King, A. G. Myelosuppression and kinase selectivity of multikinase angiogenesis inhibitors. *Br. J. Cancer* **2009**, *101*, 1717–1723.
(40) Bae, J. H.; Ravindranathan, K. P.; Mandiyan, V.; Ekkati, A. R.; Schlessinger, J.; Jorgensen, W. L. Protein Data Bank ID 3JS2.
(41) Irwin, J. J.; Shoichet, B. K. ZINC-a free database of commercially available compounds for virtual screening. *J. Chem. Inf. Model.* **2005**, *45*, 177–182.
(42) Friesner, R. A.; Banks, J. L.; Murphy, R. B.; Halgren, T. A.; Klicic, J. J.; Mainz, D. T.; Repasky, M. P.; Knoll, E. H.; Shelley, M.; Perry, J. K.; Shaw, D. E.; Francis, P.; Shenkin, P. S. Glide: A New Approach for Rapid, Accurate Docking and Scoring. 1. Method and Assessment of Docking Accuracy. *J. Med. Chem.* **2004**, *47*, 1739–1749.
(43) Friesner, R. A.; Murphy, R. B.; Repasky, M. P.; Frye, L. L.; Greenwood, J. R.; Halgren, T. A.; Sanschagrin, P. C.; Mainz, D. T. Extra Precision Glide: Docking and Scoring Incorporating a Model of Hydrophobic Enclosure for Protein-Ligand Complexes. *J. Med. Chem.* **2006**, *49*, 6177–6196.
(44) (a) Jorgensen, W. L.; Maxwell, D. S.; Tirado-Rives, J. Development and testing of the OPLS all-atom force field on conformational energetics and properties of organic liquids. *J. Am. Chem. Soc.* **1996**, *118*, 11225–11236. (b) Jorgensen, W. L.; Tirado-Rives, J. Potential energy functions for atomic-level simulations of water and organic and biomolecular systems. *Proc. Nat. Acad. Sci U.S.A.* **2005**, *102*, 6665–6670.
(45) Muegge, I.; Enyedy, I. J. Virtual Screening for Kinase Targets. *Curr. Med. Chem.* **2004**, *11*, 693–707.
(46) Lyne, P. D.; Kenny, P. W.; Cosgrove, D. A.; Deng, C.; Zabludoff, S.; Wendoloski, J. J.; Ashwell, S. Identification of Compounds with Nanomolar Binding Affinity for Checkpoint Kinase-1 Using Knowledge based Virtual Screening. *J. Med. Chem.* **2004**, *47*, 1962–1968.
(47) Singh, J.; Chuaqui, C. E.; Boriack-Sjodin, P. A.; Lee, W.; Pontz, T.; Corbley, M. J.; Cheung, H. K.; Arduini, R. M.; Mead, J. N.; Newman, M. N.; Papadatos, J. L.; Bowes, S.; Josiah, S.; Ling, L. E. Successful Shape Based Virtual Screening: The Discovery of a Potent Inhibitor of the Type I TGF B Receptor Kinase (TBR1). *Bioorg. Med. Chem. Lett.* **2003**, *13*, 4355–4359.
(48) Manetti, F.; Botta, M. Small-Molecule Inhibitors of Fibroblast Growth Factor Receptor (FGFR) Tyrosine Kinases (TK). *Curr. Pharm. Des.* **2003**, *9*, 567–581.
(49) Stamos, J.; Sliwkowski, M. X.; Eigenbrot, C. Structure of the Epidermal Growth Factor Receptor 2 Kinase Domain Alone and in Complex with 3,4-Anilioquinazoline Inhibitor. *J. Biol. Chem.* **2002**, *277*, 46265–46272.
(50) Hubbard, S. R. Crystal structure of the activated insulin 2 receptor tyrosine kinase in complex with peptide 3 substrate and ATP analog. *EMBO J.* **1997**, *16*, 5572–5582.
(51) Hasegawa, M.; Nishigaki, N.; Washio, Y.; Kano, K.; Harris, P. A.; Sato, H.; Mori, I.; West, R. I.; Shibahara, M.; Toyoda, H.; Wand, L.; Nolte, R. T.; Veal, J. M.; Cheung, M. Discovery of Novel Benzimadazoles as Potent Inhibitors of TIE-2 and VEGFR-2 Tyrosine Kinase Receptors. *J. Med. Chem.* **2007**, *50*, 4453–4470.
(52) Hennequin, L. F.; Allen, J.; Breed, J.; Curwen, J.; Fennell, M.; Green, T. P.; Lambert-Van der Brempt, C.; Morgentin, R.; Norman, R. A.; Oliver, A.; Otterbein, L.; Ple, P. A.; Warin, N.; Costello, G. *N*-(5-Chloro-1,3-benzodioxol-4-yl)-7-[2-(4-methylpiperazin-1-yl)ethoxy]-5-(tetrahydro-2*H*-pyran-4-yloxy) quinazolin-4-amine, a novel, highly selective, orally available, dual-specific c-src/abl kinase inhibitor. *J. Med. Chem.* **2006**, *49*, 6465–6488.
(53) Wang, Z.; Canagarajah, J .; Boehm, J. C.; Kassisa, S.; Cobb, M. H.; Young, P. R.; Abdel-Meguid, S.; Adams, J. L.; Goldsmith, E. J. Structural Basis of Inhibitor Selectivity in Map Kinases. *Structure* **1998**, *6*, 1117–1128.
(54) Jorgensen, W. L.; Tirado-Rives, J. Molecular Modeling of Organic and Biomolecular Systems using BOSS and MCPRO. *J. Comput. Chem.* **2005**, *26*, 1689–1700.
(55) Furdui, C. M.; Lew, E. D.; Schlessinger, J.; Anderson, K. S. Autophosphorylation of FGFR1 Kinase is Mediated by a Sequential and Precisely Ordered Reaction. *Mol. Cell* **2006**, *21*, 711–717.
(56) Mohammadi, M.; Schlessinger, J.; Hubbard, S. R. Structure of the FGF receptor tyrosine kinase domain reveals a novel autoinhibitory mechanism. *Cell* **1996**, *86*, 577–587.
(57) Nichols, S. E.; Domaoal, R. A.; Thakur, V. V.; Bailey, C. M.; Wang, L.; Tirado-Rives, J.; Anderson, K. S.; Jorgensen, W. L. Discovery of Wild-type and Y181C Mutant Non-nucleoside HIV-1 Reverse Transcriptase Inhibitors Using Virtual Screening with Multiple Protein Structures. *J. Chem. Inf. Model.* **2009**, *49*, 1272–1279.
(58) Barreiro, G.; Kim, J. T.; Guimarães, C. R. W.; Bailey, C. M.; Domaoal, R. A.; Wang, L.; Anderson, K. S.; Jorgensen, W. L. From Docking False-Positive to Active Anti-HIV Agent. *J. Med. Chem.* **2007**, *50*, 5324–5329.
(59) Jorgensen, W. L. Efficient Drug Lead Discovery and Optimization. *Acc. Chem. Res.* **2009**, *42*, 724–733.
(60) Jorgensen, W. L. *QikProp*, version 3.0; Schrodinger, LLC: New York, 2006.
(61) Thakur, V. V.; Kim, J. T.; Hamilton, A. D.; Bailey, C. M.; Domaoal, R. A.; Wang, L.; Anderson, K. S.; Jorgensen, W. L. Optimization of pyrimidinyl- and triazinyl-amines as non-nucleoside inhibitors of HIV-1 reverse transcriptase. *Bioorg. Med. Chem. Lett.* **2006**, *16*, 5664–5667.
(62) Leach, A. R.; Shoichet, B. K.; Peishoff, C. E. Prediction of Protein−Ligand Interactions. Docking and Scoring: Successes and Gaps. *J. Med. Chem.* **2006**, *49*, 5851–5855.